SECOND EUROPEAN CONFERENCE ON EARTHQUAKE ENGINEERING
AND SEISMOLOGY, ISTANBUL AUG. 25-29, 2014

SEISMIC ANALYSIS OF HYBRID ROCKING BRIDGE BENTS

Anastasios I. GIOUVANIDIS[1], *Elias G. DIMITRAKOPOULOS[2]

ABSTRACT

Current (code-based) seismic bridge design focuses on accommodating structural deformation, and eventually damage, during an earthquake excitation. On the contrary, a rocking bridge pier/bent is designed to uplift and pivot, in order to limit structural deformation and damage. A rocking bridge utilizes primarily its rotational inertia to counter the seismic demand. This paper investigates, analytically and numerically, the seismic response of a symmetric rocking bridge bent/frame. In particular, it examines both free-standing and hybrid (i.e. enhanced with supplemental damping and re-centering capacity) symmetric rocking bridge bents. The paper neglects the structural deformation of the frame-members and establishes the equations of motion following the principles of analytical dynamics. The analysis considers both pulse-type and non-pulse-type ground motions. It illustrates the sensitivity of the response to the fracture elongation of the supplemental re-centering and damping devices. The results confirm the high-performance seismic behavior of the (hybrid) rocking frame.

Keywords: rocking bridges, structural dynamics, seismic resistant structures, analytical dynamics, prefabricated bridges

INTRODUCTION

Rocking isolation hinges on allowing the bridge piers to uplift and pivot during an earthquake excitation. Thus, this alternative seismic design focuses on diminishing structural deformation and damage, and is currently proliferating. Of particular interest in this context, is the structural configuration of the '*rocking frame*' (Fig. 1).

The '*rocking frame*' combines the merits of the precast construction method (see Pang et al. (2008), Wacker et al. (2005) and references therein), with the benefits of rocking isolation. Mander and Cheng (1997) proposed the rocking bridge bent (rocking frame) as a 'damage avoidance design' for bridges. Makris and Vassiliou (2012) revisited the seismic response of the '*rocking frame*'. They showed that the more 'top-heavy' the rocking frame is the more stable it becomes. DeJong and Dimitrakopoulos (2014) established a methodology to define, an exact or approximate, equivalence between more complicated rocking structures (e.g. the rocking wall, the asymmetric rocking frame and the rocking arch) and the archetypal rocking block. Recently, Dimitrakopoulos and Giouvanidis (2014) investigated the seismic stability of the asymmetric rocking frame and showed its high-performance

[1] Post-graduate Student, Department of Civil & Environmental Engineering, The Hong Kong University of Science and Technology, Kowloon Bay, Hong Kong, e-mail: agiouvanidis@ust.hk
[2]*Corresponding author, Assistant Professor, Department of Civil & Environmental Engineering, The Hong Kong University of Science and Technology, Kowloon Bay, Hong Kong, e-mail: ilias@ust.hk

seismic behavior.

Currently, 'rocking' bridges exist in New Zealand, e.g. the Rangitikei Railway Bridge and the Deadman's Point Bridge at Cromwell (Priestley et al. 1996, Skinner et al. 1980) and date back to the 80's. During the last ten years though, many experiments have verified the beneficial isolation effect of the rocking behavior (Solberg et al. 2009, Cheng 2008, Chen et al. 2006). Sakai and Mahin (2004) showed that rocking combined with additional re-centering capacity, can reduce significantly the (seismic) residual displacements/deformations of a bridge pier, without altering substantially its peak response. Further, the addition of supplemental energy dissipation confines the amplitude of rocking and has been proposed, or considered for rocking bridges among others by Antonellis and Panagiotou (2013), Marriott et al. (2009), Palermo et al. (2007), Palermo et al. (2005). Dimitrakopoulos and DeJong (2012a) performed a thorough study on the effect of viscous damping on rocking response. The combined use of supplemental damping and additional re-centering devices leads to hybrid rocking bridges that attracted the attention of researchers (Kam et al. (2010), Marriott et al. (2009), Palermo et al. (2007), Palermo et al. (2005) among others) as 'high-performance systems' that could survive major earthquakes without significant damage. In this context, there is an increasing need to examine the rocking response and assess the seismic stability of rocking bridge bents.

The present study, focuses on the *symmetric rocking frame* and builds on previous work (Makris and Vassiliou 2012, DeJong and Dimitrakopoulos 2014, Dimitrakopoulos et al. 2013) by assessing the seismic stability and performance of the rocking frame, free-standing or hybrid. The study also evaluates the effect of basic design parameters from the standpoint of potential future bridge applications. Specifically, it examines the effect of different levels of supplemental viscous damping and elastic stiffness, as well as the assumed fracture elongation (of the supplemental re-centering and damping devices) on the seismic response of the rocking bent.

ANALYTICAL MODELLING OF THE HYBRID ROCKING FRAME

Consider a rocking frame free-standing, or (hybrid) strengthened with central unbonded tendons and external viscous dampers at the bottom of the piers (Fig. 1). Assume that sliding at the contact surfaces is restricted and ignore the deformation of the (three) members. During a strong ground motion, this rocking frame develops a three-block rocking mechanism as in Fig. 1.

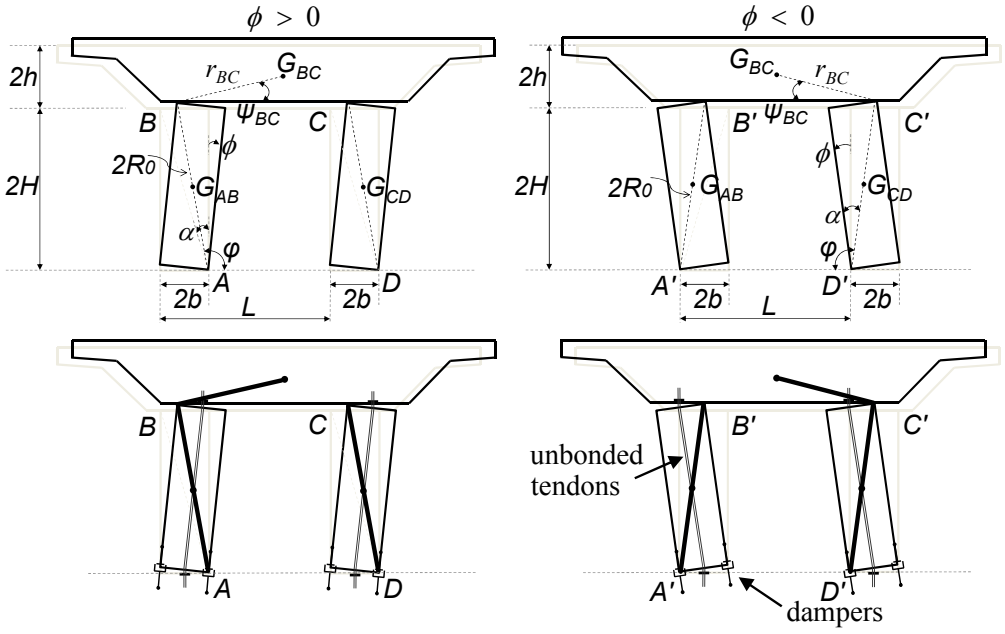

Fig. 1 The examined rocking bridge bent

Kinematics

Fig. 1 shows the assumed three-block mechanism for both clockwise and counter-clockwise rotations and the pertinent pivot points A, B, C, D and A', B', C', D' accordingly. The two columns exhibit the same rocking rotation and the connecting cap-beam sustains only rigid body translation.

The kinematics of the three block mechanism of Fig. 1 can be captured with a single generalized coordinate, the angle φ (Fig. 1) with respect to the *x*-axis. The pertinent rocking amplitude is the rotation ϕ with respect to the initial (rest) position: $\phi = \varphi_0 - \varphi$ (Fig. 1).

Equation of motion during rocking

The equation of motion for the rocking mechanism of Fig. 1 is derived using Lagrange's equation:

$$\frac{d}{dt}\left(\frac{\partial T}{\partial \dot{\varphi}}\right) - \frac{\partial T}{\partial \varphi} + \frac{\partial V}{\partial \varphi} = Q \tag{1}$$

Where T is the kinetic energy, V is the potential energy, Q is the generalized force and φ is the generalized coordinate which describes the rocking motion.

The potential energy of the three-block mechanism can be expressed as:

$$V = V_{fr} + V_{tend} \tag{2}$$

Where V_{fr} is the potential energy of the free-standing frame (due to the gravitational forces) and V_{tend} is the additional potential energy due to the elongation of the tendons. It holds:

$$V_{fr} = \left[2\left(m_{AB} + m_{BC}\right) R_0 \sin\varphi + m_{BC} r_{BC} \sin\psi_{BC}\right] g \tag{3}$$

And:

$$V_{tend} = 4k\left(\delta l\right)^2 \tag{4}$$

Where m_{AB}, m_{BC} and m_{CD} are the masses of the members AB, BC and CD, respectively and δl the elongation of the tendon. Therefore:

$$V_{tend} = 8kb^2\left[1 + \sin\left(\alpha - \varphi\right)\right] \tag{5}$$

Ignoring the mass of the tendons and the dampers, the kinetic energy of the system is:

$$T = \left(I_{AB} + 2m_{BC}R_0^2\right)\dot{\varphi}^2 \tag{6}$$

Where I_{AB} is the mass moment of inertia of AB with respect to the pivot point A (or A') and R_0 is the half length of the diagonal of the AB column of the frame (Fig. 1).

The calculation of the virtual work of the non-conservative forces yields the generalized forces:

$$\delta W_{nc} = Q\delta\varphi \tag{7}$$

Or:

$$\delta W_G + \delta W_D = \left(Q_G + Q_D\right)\delta\varphi \tag{8}$$

Where the generalized inertia force Q_G is:

$$Q_G = -2\left(m_{AB} + m_{BC}\right) R_0 \sin\varphi \ddot{u}_g \tag{9}$$

And the generalized damping force Q_D is:

$$Q_D = -4Cb^2\left[1 - \sin\left(\alpha - \varphi\right)\right]\dot{\varphi} \tag{10}$$

C is the damping constant of the linear external viscous dampers. After substituting into Lagrange's equation (Eq. (1)), the equation of motion can be written as (Makris and Vassiliou 2012, DeJong and Dimitrakopoulos 2014, Dimitrakopoulos et al. 2013):

$$I_{nl}\left(\varphi\right)\ddot{\varphi} - G_{nl}\left(\varphi\right)g + K_{nl}\left(\varphi\right) + D_{nl}\left(\varphi\right)\dot{\varphi} = -B_{nl}\left(\varphi\right)\ddot{u}_g \tag{11}$$

Where I_{nl}, G_{nl}, B_{nl}, K_{nl} and D_{nl} are nonlinear functions of the generalized coordinate and equal with:

$$
\begin{aligned}
I_{nl}(\varphi) &= 2(I_0 + 2m_{BC}R_0^{\,2}) \\
G_{nl}(\varphi) &= -2\left(m_{AB} + m_{BC}\right)R_0\cos\varphi \\
B_{nl}(\varphi) &= 2\left(m_{AB} + m_{BC}\right)R_0\sin\varphi \\
K_{nl}(\varphi) &= -8kb^2\cos\left(\alpha - \varphi\right) \\
D_{nl}(\varphi) &= 4Cb^2\left[1 - \sin\left(\alpha - \varphi\right)\right]
\end{aligned}
\tag{12}
$$

For the symmetric rocking frame the minimum dimensionless ground acceleration capable of initiating rocking is $\lambda = \ddot{u}_{g,\min} / g = \tan\alpha$. The study assumes that the behavior of the supplemental tendons and dampers is elastic until fracture, which occurs simultaneously for all tendons and dampers. Hence, if the tendons and the dampers reach their fracture elongation ε_f, say at time instant t_f, the equation of motion switches irreversibly to the equation of the free-standing frame (Eq. (14), (15)) (terms K_{nl} and D_{nl} in Eq. (11) disappear).

Further, following Makris and Zhang (2001) work, we define:

$$
\begin{aligned}
q &= \frac{p^2 u_f}{g} \\
\sigma &= \frac{F_u}{\left(m_{AB} + m_{BC}\right)g} \\
\gamma &= \frac{3Cb^2}{2\left(m_{AB} + \frac{3}{2}m_{BC}\right)pR_0^{\,2}}
\end{aligned}
\tag{13}
$$

Where q is the influence factor, σ is the strength parameter in which F_u is the strength of the tendon and γ is a dimensionless group (Dimitrakopoulos and DeJong 2012a) relating the damping constant C with the masses m_{AB}, m_{BC} and with the frequency parameter $p = \sqrt{3g / 4R_0}$ of the symmetric rocking frame.

Substituting Eq. (12) into Eq. (11) and with the aid of the abbreviations of Eq. (13) we finally derive the equations which describe the motion of the symmetric rocking frame with respect to the generalized coordinate φ before and after brittle fracture occurs (Eq. (14)).

$$
\ddot{\varphi} = \begin{cases}
-p^2\left(\dfrac{m_{AB} + m_{BC}}{m_{AB} + \frac{3}{2}m_{BC}}\right)\left[\cos\varphi + \sin\varphi\dfrac{\ddot{u}_g}{g} - 3\dfrac{\sigma}{q}\sin^2\alpha\cdot\cos\left(\alpha - \varphi\right)\right] - p\cdot\gamma\left[1 - \sin\left(\alpha - \varphi\right)\right]\dot{\varphi}, & if\ t < t_f \\
-p^2\left(\dfrac{m_{AB} + m_{BC}}{m_{AB} + \frac{3}{2}m_{BC}}\right)\left[\cos\varphi + \sin\varphi\dfrac{\ddot{u}_g}{g}\right], & if\ t > t_f
\end{cases}
\tag{14}
$$

The equations of motion written also in terms of the rocking amplitude ϕ are:

$$
\ddot{\phi} = \begin{cases}
-p^2\left(\dfrac{m_{AB} + m_{BC}}{m_{AB} + \frac{3}{2}m_{BC}}\right)\left[\sin\left(\alpha - \phi\right) - \cos\left(\alpha - \phi\right)\dfrac{\ddot{u}_g}{g} + 3\dfrac{\sigma}{q}\sin^2\alpha\cdot\sin\phi\right] - p\cdot\gamma\left(1 + \cos\phi\right)\dot{\phi}, & if\ t < t_f \\
-p^2\left(\dfrac{m_{AB} + m_{BC}}{m_{AB} + \frac{3}{2}m_{BC}}\right)\left[\sin\left(\alpha - \phi\right) - \cos\left(\alpha - \phi\right)\dfrac{\ddot{u}_g}{g}\right], & if\ t > t_f
\end{cases}
\tag{15}
$$

Eq. (15) gives the equations of motion with respect to the rocking rotation ϕ, before and after brittle fracture occurs. Note the equivalence between the equations describing the motion of the symmetric rocking frame (Eq.(15)) with the pertinent equations of the rocking block (Dimitrakopoulos and DeJong 2012a).

To determine the post-impact state, we need first to solve the rocking-impact problem and determine the angular velocity after the impact. An in-depth analysis for different geometries of the rocking frame can be found in the work of Dimitrakopoulos and Giouvanidis (2014). Herein, the effect of impact is captured simply with the ratio of the angular velocities after and before the impact, defined as the coefficient of restitution $\varepsilon = \dot{\varphi}^{+} / \dot{\varphi}^{-}$:

$$\varepsilon = \frac{\dot{\varphi}^{+}}{\dot{\varphi}^{-}} = \frac{1 - \frac{3}{2}\sin^2\alpha + 3\gamma\cos 2\alpha}{1 + 3\gamma} \tag{16}$$

Where $\gamma = \frac{m_{BC}}{2m_{AB}}$, $\cos\alpha = \frac{H}{R_0}$, and $\sin\alpha = \frac{b}{R_0}$, verifying the result derived recently by Makris and Vassiliou (2012).

ASSESSMENT OF THE SEISMIC STABILITY OF THE SYMMETRIC ROCKING FRAME

This section investigates the seismic response of a symmetric (free-standing and hybrid) rocking frame. Consider a typical span of a multiple-span highway bridge, with a cross section as in Fig. 1, and assume a deck *13 m* wide and a deck-cap-beam with height *2h = 2 m*. The bent consists of two columns with *2b = 1.0 m* base each, and height *2H = 7.0 m*, while the distance between them is *L = 8 m*. The deck/piers mass ratio is *10*, corresponding roughly to a span of *40 m* length (Mander and Cheng 1997). The polar radius of gyration of the deck cross-section is assumed to be *3.58 m* and the distance from the center of mass of the deck-cap-beam to the pivot points is r_{BC} *= 4.64 m* (Fig. 1). Finally, the beam-column and the column-foundation connections prevent relative sliding, but allow uplifting and consequently act as simple/free supports.

Mathematical (pulse-type) ground motions

Large rocking structures (e.g. a rocking bridge bent) are more vulnerable to low-frequency coherent ground motions (e.g. Acikgoz and DeJong (2013) and references therein). Hence, to assess the seismic stability of the rocking bridge bent we examine first pulse-type excitations. Various mathematical pulses have been proposed in the literature that can capture both qualitatively and quantitatively the long distinct pulses of near-fault ground motions (Acikgoz and DeJong 2013, Kafle et al. 2011, Voyagaki et al. 2013). In this study, we consider the Ricker pulse (Ricker 1944, 1943) which can be defined with two parameters: either the acceleration (a_g) or the velocity (v_g) amplitude, and the period T_g. Eq. (17) describes the symmetric Ricker pulse:

$$\ddot{u}_g(t) = a_g\left(1 - \frac{2\pi^2 t^2}{T_g^2}\right)e^{-\frac{1}{2}\frac{2\pi^2 t^2}{T_g^2}} \tag{17}$$

Similarly, Eq. (18) gives the antisymmetric Ricker pulse:

$$\ddot{u}_g(t) = \frac{a_g}{\beta}\left(\frac{4\pi^2 t^2}{3T_g^2} - 3\right)\frac{2\pi t}{\sqrt{3}T_g}e^{-\frac{1}{2}\frac{4\pi^2 t^2}{3T_g^2}} \tag{18}$$

In both cases (Eq. (17) and (18)) $T_g = 2\pi / \omega_g$ is the period that maximizes the Fourier spectrum of the corresponding Ricker wavelet. In Eq. (18), $\beta = 1.38$ enforces the function to have a maximum equal to the acceleration amplitude a_g.

The consideration of pulse-type excitations facilitates also the use of dimensionless variables

(e.g. DeJong and Dimitrakopoulos (2014), Dimitrakopoulos and DeJong (2012b)). Herein, the following results are presented in dimensionless terms scaled with respect to the rocking properties (frequency parameter p and slenderness α) of a column of the frame.

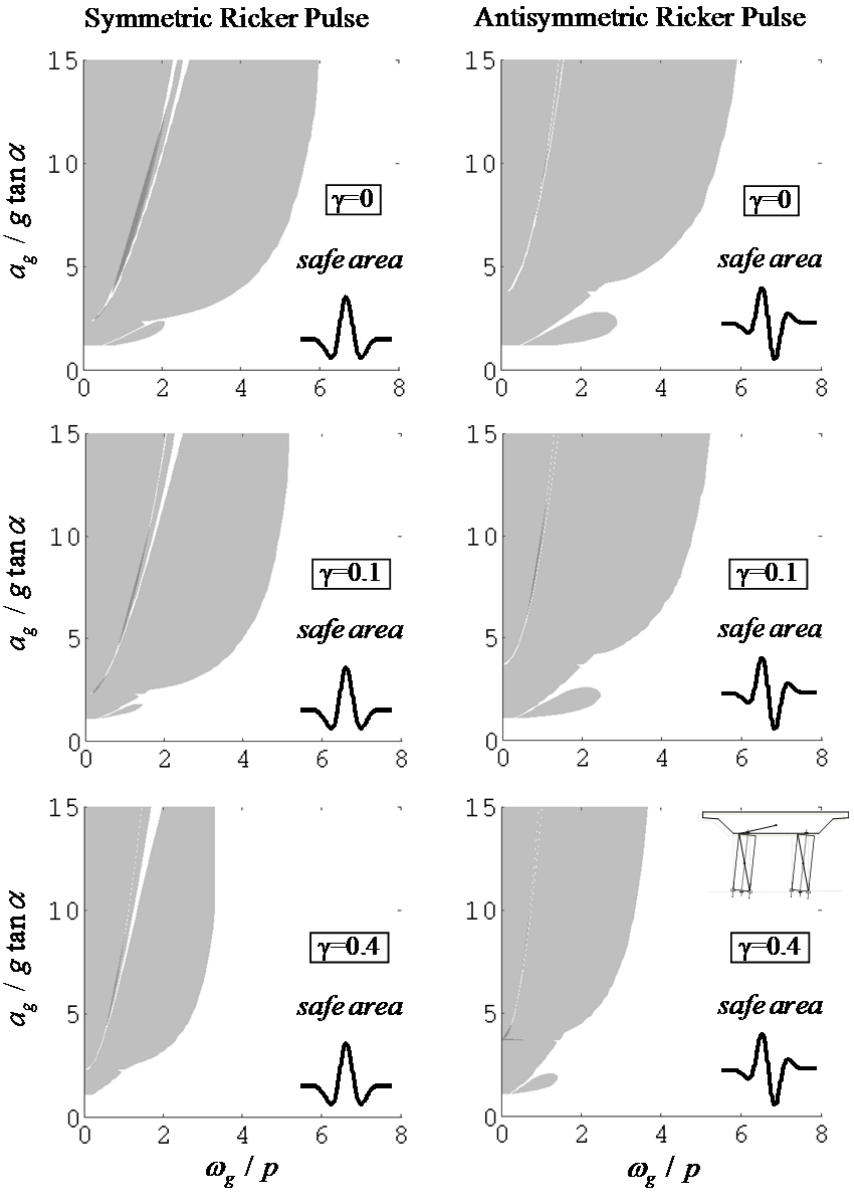

Fig. 2 Overturning plots of the symmetric free-standing ($\gamma = 0$) and of the damped rocking frame with additional damping γ equal to $0.1, 0.4$

To limit the amplitude of rocking rotations and enhance the seismic stability of the rocking bridge bent, we investigate the use of unbonded (slack) central tendons and external viscous dampers (Fig. 1); thus, converting the free-standing into a hybrid rocking frame. As a first approach, we investigate separately the effect of each one (i.e. parameters σ and γ) on the seismic stability of the symmetric rocking bridge bent. Further, to highlight the high-seismic-performance of the hybrid frame, we examine the combined effect of the parameters σ and γ, which control the stiffness and damping constants respectively (Eq. ((13)), on the response.

The overturning plot (e.g. of Fig. 2) separates the control plane (a_g/(g tanα) - ω_g/p) into two areas: a shaded (grey) area where the structure overturns (after impact or without any preceding impact)

and a non-shaded (white) area, where the structure is safe (no overturning occurs). Recall that rocking structures display various overturning modes with respect to the number of the preceding impacts (Dimitrakopoulos and DeJong 2012b). Fig. 2 shows that the structure is most vulnerable to low-frequency acceleration pulses, while it survives even high amplitude higher-frequency pulses. In other words, the seismic response of the rocking frame exhibits typical, and in that sense, predictable rocking behavior under pulse-type excitations (Dimitrakopoulos and DeJong 2012b).

Fig. 2 compares the seismic stability of the free-standing ($\sigma=0$ and $\gamma=0$) rocking frame and the rocking frame which is retrofitted with external viscous dampers, both subjected to the same Ricker pulses. It examines a range of dimensionless damping values ($\gamma=0.1$, $\gamma=0.4$), which correspond to damping constants equal to *12.6 MNs/m* and *50.6 MNs/m* respectively.

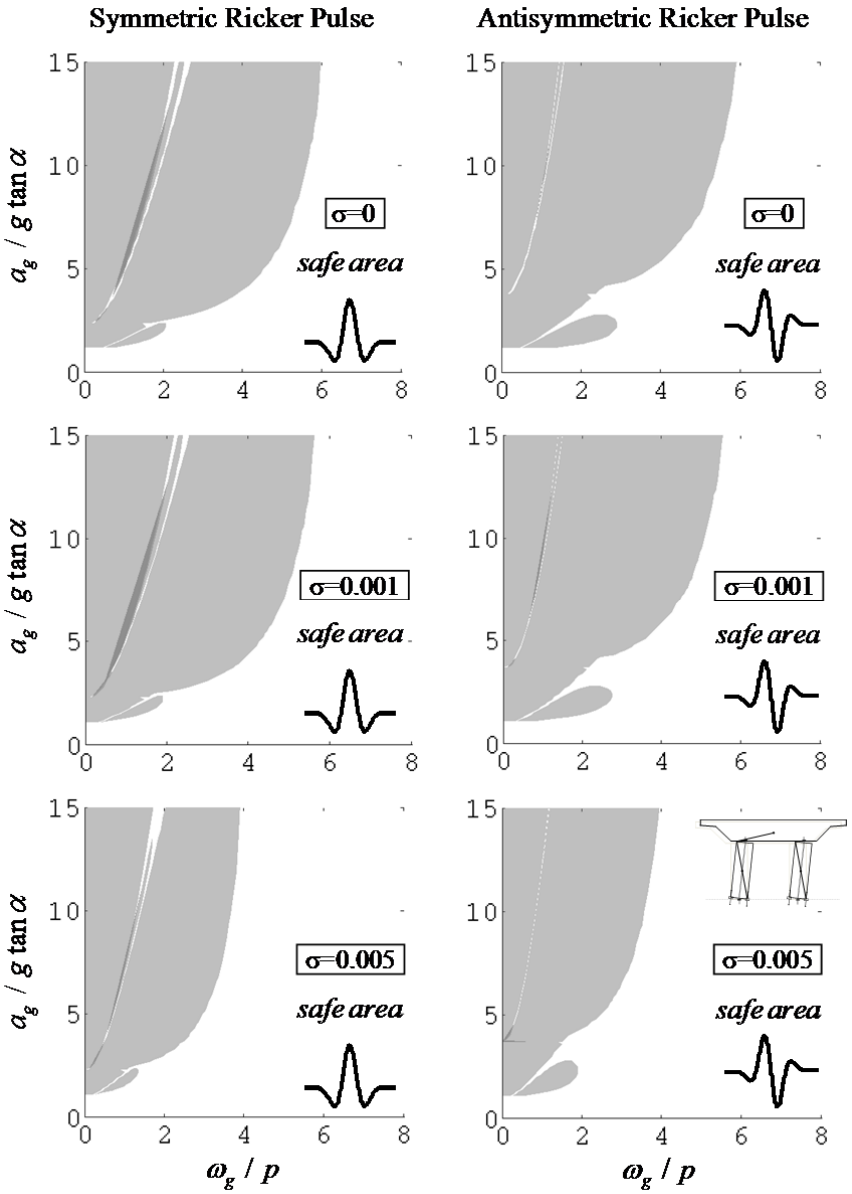

Fig. 3 Overturning plots of the symmetric free-standing ($\sigma = 0$) rocking frame and of the frame retrofitted with a central tendon assuming no fracture with strength parameter σ equal to *0.001, 0.005*

Further, Fig. 3 displays the seismic response of the rocking frame enhanced solely with central tendons, which are assumed linear-elastic. The dimensionless strength parameters considered are

$\sigma=0.001$ and $\sigma=0.005$, which correspond to stiffness constants equal with $7.24\ MN/m$ and $36.2\ MN/m$ respectively. Both figures (Fig. 2 and Fig. 3) demonstrate the enhanced seismic performance of the hybrid frame, supplemented with either damping or re-centering capacity.

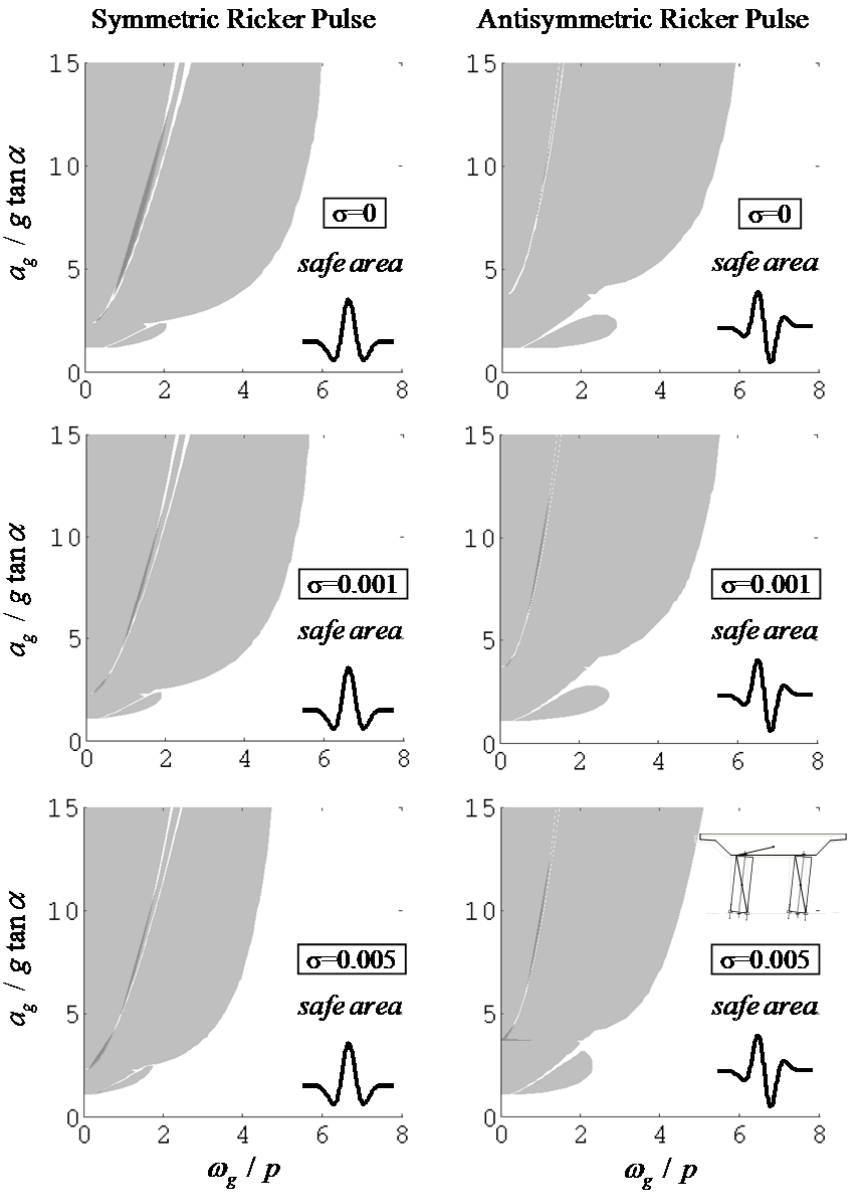

Fig. 4 Overturning plots of the symmetric free-standing ($\sigma = 0$) rocking frame and of the frame retrofitted with a central tendon considering fracture elongation $\varepsilon_f = 1\%$ with strength parameter σ equal to 0.001, 0.005

As a second step, we assume that the tendons remain linear-elastic until their brittle fracture at elongation ε_f. The critical rocking rotation, beyond which the structure becomes unstable, and potentially overturns, is $\phi_{cr} = \alpha$. Consequently, rotations of the hybrid frame near overturning correspond, roughly, to elongations of the tendon in the order of 1.0% (assuming a tendon with length equal to $8.5\ m$ as in Mander and Cheng (1997)).

Fig. 4 presents the seismic stability of the free-standing rocking frame and the frame enhanced with central tendons considering $\varepsilon_f = 1\%$ fracture elongation. In particular, in Fig. 3 ε_f is high enough to ensure the system of tendons stays within the linear-elastic range until overturning, whereas in Fig. 4 the fracture elongation is taken as $\varepsilon_f = 1.0\%$ the length of the tendon. When the elongation of the

tendon exceeds the fracture limit we assume that, from that point on, the frame behaves as free-standing.

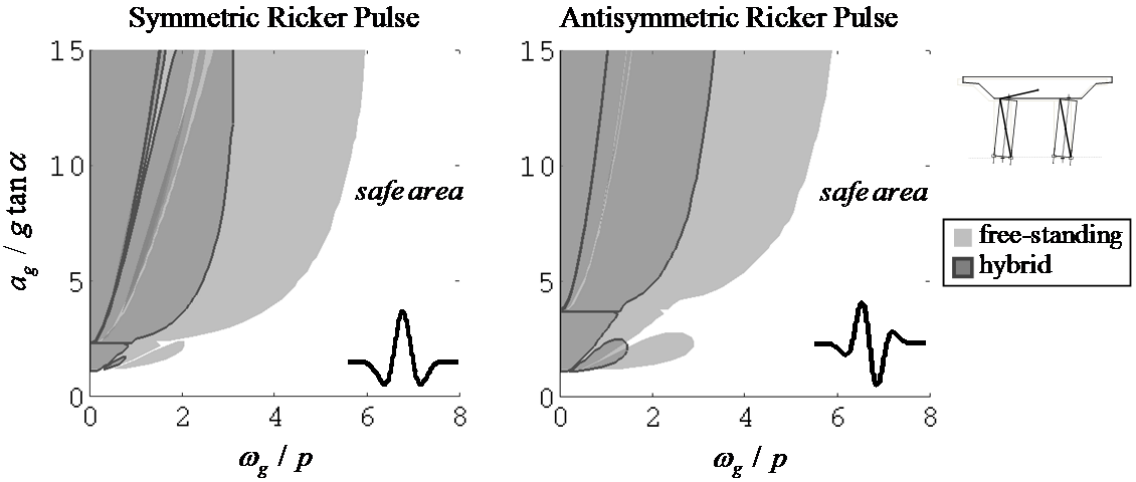

Fig. 5 Overturning plots of the symmetric free-standing ($\sigma = 0$, $\gamma = 0$) and hybrid rocking frame assuming no fracture with stiffness and damping parameters σ and γ equal to *0.005, 0.1* respectively

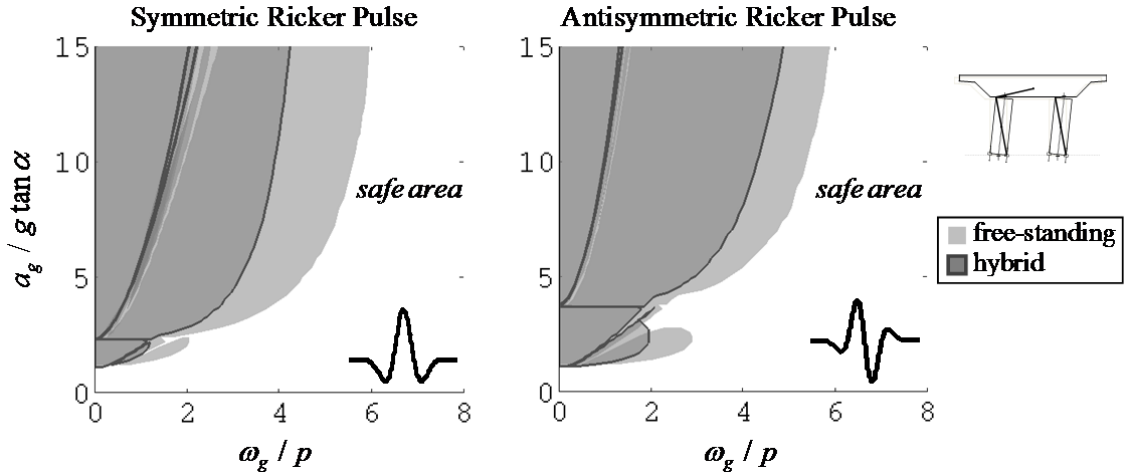

Fig. 6 Overturning plots of the symmetric free-standing ($\sigma=0$, $\gamma=0$) and hybrid rocking frame considering fracture elongation $\varepsilon_f = 1\%$ with stiffness and damping parameters σ and γ equal to *0.005, 0.1* respectively

Finally, we study the rocking bridge bent enhanced with central tendons and external viscous dampers combined. Fig. 5 and Fig. 6 show the seismic behavior of both free-standing and hybrid rocking frames under pulse-type excitations. Fig. 5 corresponds to the case the system of tendons and dampers remain linear-elastic without fracture, whereas in Fig. 6 after a certain elongation both the tendons and the dampers fail simultaneously. The comparison of Fig. 5 and Fig. 6 unveils the sensitivity of the seismic performance/stability to the assumed fracture elongation. In general, the higher the fracture elongation the more drastic the enhancement of the stability (Fig. 5, Fig. 6) is. Interestingly though, the seismic stability of the hybrid is not always better compared with the free-standing rocking frame. Similar to the anchored rocking block (Dimitrakopoulos and DeJong 2012a) and to the asymmetric rocking frame (Dimitrakopoulos and Giouvanidis 2014), counter results also appear where the response of the hybrid frame is worse than that of the corresponding free-standing frame. Fig. 2 to Fig. 6 illustrate such cases, wherein the hybrid frame overturns while the free-standing frame survives the excitation; for instance when $a_g/(g\tan\alpha) \approx 1 \div 3$, $\omega_g/p \approx 1 \div 2$ and the excitation is an antisymmetric Ricker pulse (Fig. 6). These peculiar response characteristics stem from the frail (highly nonlinear) nature of rocking dynamics and in that sense are anticipated.

Historic Excitations

To extend the seismic stability analysis of the rocking frame, we examine historic excitations regardless of whether they contain distinguishable pulses or not. In particular, we consider a well-known set of historic ground motions scaled to yield a probability of exceedance of *2%* in *50* years (SAC 1997).

Table 1 Earthquake records (probability of exceedance of *2%* in *50* years) (SAC 1997)

Number	Record	Magni-tude	Scale Factor	DT (s)	Duration (s)	PGA (cm/sec^2)
SE21	1992 Mendocino	7.1	0.98	0.02	59.98	741.13
SE22	1992 Mendocino	7.1	0.98	0.02	59.98	476.22
SE23	1992 Erzincan	6.7	1.27	0.005	20.775	593.60
SE24	1992 Erzincan	6.7	1.27	0.005	20.775	529.06
SE25	1949 Olympia	6.5	4.35	0.02	79.98	878.23
SE26	1949 Olympia	6.5	4.35	0.02	79.98	805.68
SE27	1965 Seattle	7.1	10.04	0.02	81.82	1722.40
SE28	1965 Seattle	7.1	10.04	0.02	81.82	1364.70
SE29	1985 Valpariso	8.0	2.9	0.025	99.975	1605.50
SE30	1985 Valpariso	8.0	2.9	0.025	99.975	1543.50
SE31	1985 Valpariso	8.0	3.96	0.025	99.975	1246.20
SE32	1985 Valpariso	8.0	3.96	0.025	99.975	884.43
SE35	1978 Miyagi-oki	7.4	1.78	0.02	79.98	595.07
SE36	1978 Miyagi-oki	7.4	1.78	0.02	79.98	768.62

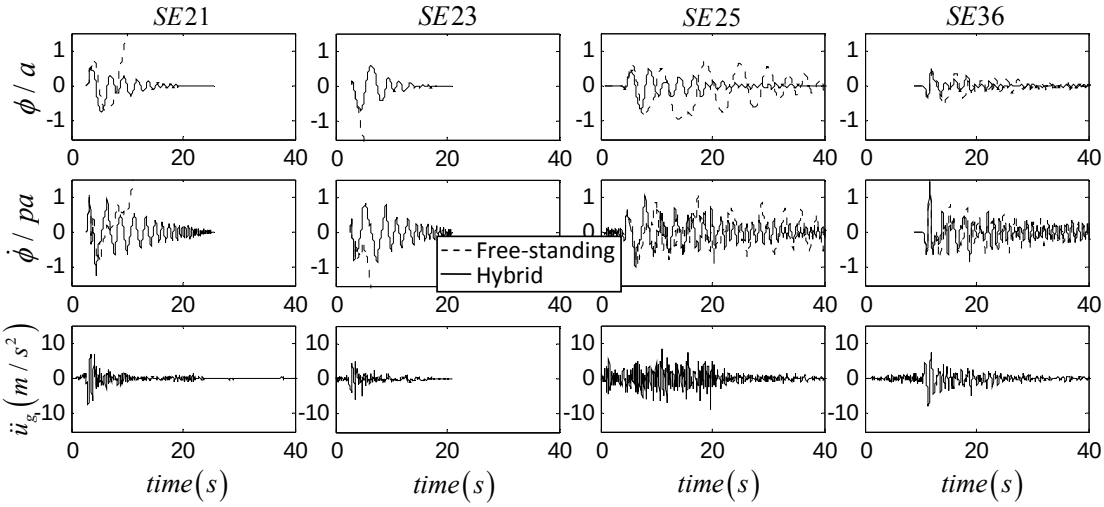

Fig. 7 Seismic response of the symmetric (free-standing and hybrid) rocking frame for different earthquake records (bottom). Top: dimensionless rocking rotation and middle: dimensionless angular velocity

Fig. 7 and Fig. 8 compare the seismic response of the free-standing and hybrid rocking frames, in terms of time-history and peak response respectively. For the hybrid frame a fracture elongation of $\varepsilon_f = 1.0\%$ is assumed. Fig. 8 shows that among the examined historic records the most destructive are the SE23, SE24 from the 1992 Erzican, Turkey earthquake, the SE21 from the 1992 Mendocino, California earthquake and the SE27 from the 1965 Seattle, Washington earthquake. Even though the examined ground motions are scaled to the maximum credible earthquake level, the free-standing bridge bent survives most of them, while the pertinent hybrid bent not only survives all ground motions of Table 1, but also, it does not reach the critical (fracture) rotation. Recall that, according to the assumptions of the present analysis, when the structure survives the motion (i.e. it does not overturn), it eventually re-centers to the original configuration without any permanent rotation and/or damage. Finally, note that rocking response becomes less orderly for non-coherent seismic excitations (Acikgoz and

DeJong 2013). Hence, it is precarious to derive general conclusions, for other excitations, based on the present results.

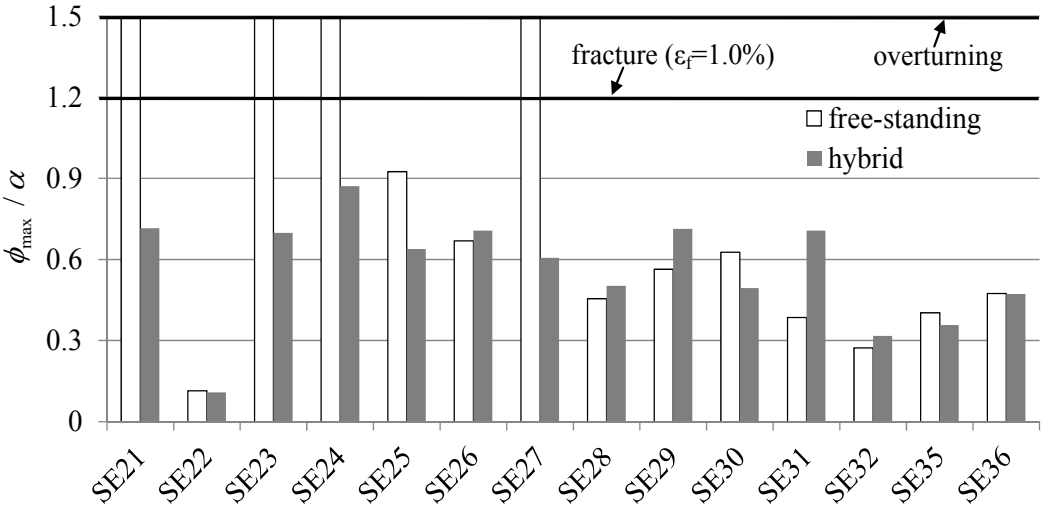

Fig. 8 Maximum rotations (in dimensionless terms) for all the earthquake records of Table 1

CONCLUSIONS

This paper examines the seismic response of a symmetric (planar) rocking frame within the context of an alternative seismic design paradigm for bridge bents. In particular, the paper compares the seismic stability of both the free-standing and the hybrid (supplemented with additional restoring and/or damping capacity) rocking bridge bent.

The results confirm the ample seismic stability of the hybrid rocking bridge bent, and verify its promising high-performance seismic behavior. The hybrid rocking frame survives all historic records examined, even though they are scaled to the 'maximum credible earthquake' level. Further, the study demonstrates the effect of different levels of supplemental viscous damping and elastic stiffness, and unveils the dominant role of the fracture elongation (of the supplemental tendons and dampers) on the seismic response of the hybrid rocking frame.

ACKNOWLEDGEMENTS

Financial support was provided by the Research Grants Council of Hong Kong, under grant reference number ECS 639613.

REFERENCES

Acikgoz S. & DeJong M. J. (2013). "*The rocking response of large flexible structures to earthquakes"*. Bulletin of Earthquake Engineering**,** 1-34.

Antonellis G. & Panagiotou M. (2013). "*Seismic Response of Bridges with Rocking Foundations Compared to Fixed-Base Bridges at a Near-Fault Site"*. Journal of Bridge Engineering.

Chen Y. H., Liao W. H., Lee C. L. & Wang Y. P. (2006). "*Seismic isolation of viaduct piers by means of a rocking mechanism"*. Earthquake engineering & structural dynamics*,* 35(6)**,** 713-736.

Cheng C.-T. (2008). "*Shaking table tests of a self-centering designed bridge substructure"*. Engineering Structures*,* 30(12)**,** 3426-3433.

DeJong M. J. & Dimitrakopoulos E. G. (2014). "*Dynamically equivalent rocking structures"*. Earthquake engineering & structural dynamics*,* (in press).

Dimitrakopoulos E. G. & DeJong M. J. (2012a). "*Overturning of retrofitted rocking structures under pulse-type excitations*". Journal of Engineering Mechanics, 138(8), 963-972.
Dimitrakopoulos E. G. & DeJong M. J. (2012b). "*Revisiting the rocking block: closed-form solutions and similarity laws*". Proceedings of the Royal Society A: Mathematical, Physical and Engineering Science, 468(2144), 2294-2318.
Dimitrakopoulos E. G., DeJong M. J. & Giouvanidis A. I. (2013). "*Seismic assessment of rocking bridge bents using an equivalent rocking block*". 2013 World Congress on Advances in Structural Engineering and Mechanics.
Dimitrakopoulos E. G. & Giouvanidis A. I. (2014). "*Seismic response analysis of the asymmetric rocking frame - analytical modelling*". Earthquake engineering & structural dynamics, (under review).
Kafle B., Lam N. T., Gad E. F. & Wilson J. (2011). "*Displacement controlled rocking behaviour of rigid objects*". Earthquake Engineering & Structural Dynamics, 40(15), 1653-1669.
Kam W. Y., Pampanin S., Palermo A. & Carr A. J. (2010). "*Self-centering structural systems with combination of hysteretic and viscous energy dissipations*". Earthquake Engineering & Structural Dynamics, 39(10), 1083-1108.
Makris N. & Vassiliou M. F. (2012). "*Planar rocking response and stability analysis of an array of free-standing columns capped with a freely supported rigid beam*". Earthquake Engineering & Structural Dynamics, 42(3), 431-449.
Makris N. & Zhang J. (2001). "*Rocking response of anchored blocks under pulse-type motions*". Journal of engineering mechanics, 127(5), 484-493.
Mander J. B. & Cheng C.-T. (1997). Seismic resistance of bridge piers based on damage avoidance design, National Center for Earthquake Engineering Research.
Marriott D., Pampanin S. & Palermo A. (2009). "*Quasi-static and pseudo-dynamic testing of unbonded post-tensioned rocking bridge piers with external replaceable dissipaters*". Earthquake Engineering & Structural Dynamics, 38(3), 331-354.
Palermo A., Pampanin S. & Calvi G. M. (2005). "*Concept and development of hybrid solutions for seismic resistant bridge systems*". Journal of Earthquake Engineering, 9(06), 899-921.
Palermo A., Pampanin S. & Marriott D. (2007). "*Design, modeling, and experimental response of seismic resistant bridge piers with posttensioned dissipating connections*". Journal of Structural Engineering, 133(11), 1648-1661.
Pang J. B., Stanton J. F. & Eberhard M. O. (2008). A Precast Concrete Bridge Bent Designed to Re-Center After an Earthquake, Washington State Department of Transportation.
Priestley M. N., Seible F. & Calvi G. M. (1996). Seismic design and retrofit of bridges, John Wiley & Sons.
Ricker N. (1943). "*Further developments in the wavelet theory of seismogram structure*". Bulletin of the Seismological Society of America, 33(3), 197-228.
Ricker N. (1944). "*Wavelet functions and their polynomials*". Geophysics, 9(3), 314-323.
SAC. (1997). *Suites of Earthquake Ground Motions* [Online]. Available: http://nisee.berkeley.edu/data/strong_motion/sacsteel/ground_motions.html [Accessed 10 January 2014.
Sakai J. & Mahin S. A. (2004). "*Mitigation of residual displacements of circular reinforced concrete bridge columns*". 13th World Conference on Earthquake Engineering.
Skinner R., Tyler R., Heine A. & Robinson W. (1980). "*Hysteretic dampers for the protection of structures from earthquakes*". Bulletin, New Zealand National Society for Earthquake Engineering, 13(1), 22-36.
Solberg K., Mashiko N., Mander J. & Dhakal R. (2009). "*Performance of a damage-protected highway bridge pier subjected to bidirectional earthquake attack*". Journal of structural engineering, 135(5), 469-478.
Voyagaki E., Psycharis I. N. & Mylonakis G. (2013). "*Rocking response and overturning criteria for free standing rigid blocks to single—lobe pulses*". Soil Dynamics and Earthquake Engineering, 46(85-95).
Wacker J. M., Hieber D. G., Stanton J. F. & Eberhard M. O. (2005). Design of precast concrete piers for rapid bridge construction in seismic regions, Washington State Department of Transportation.